Published in final edited form as:
J Neurochem. 2009 August ; 110(4): 1339–1351. doi:10.1111/j.1471-4159.2009.06224.x.

Inhibition of tau fibrillization by oleocanthal via reaction with the amino groups of tau

Wenkai Li[*,†], **Jeffrey B. Sperry**[‡], **Alex Crowe**[*], **John Q. Trojanowski**[*], **Amos B. Smith III**[‡,§], and **Virginia M.-Y. Lee**[*]

[*]Center for Neurodegenerative Disease Research, Department of Pathology and Laboratory Medicine, University of Pennsylvania School of Medicine, Philadelphia, Pennsylvania

[†]Department of Biochemistry and Molecular Biophysics, University of Pennsylvania School of Medicine, Philadelphia, Pennsylvania

[‡]Department of Chemistry, University of Pennsylvania, Philadelphia, Pennsylvania

[§]Monell Chemical Senses Center, Philadelphia, Pennsylvania

Abstract

Tau is a microtubule-associated protein that promotes microtubule assembly and stability. In Alzheimer's disease and related tauopathies, tau fibrillizes and aggregates into neurofibrillary tangles. Recently, oleocanthal isolated from extra virgin olive oil was found to display non-steroidal anti-inflammatory activity similar to ibuprofen. Since our unpublished data indicates an inhibitory effect of oleocanthal on Aβ fibrillization, we reasoned that it might inhibit tau fibrillization as well. Herein we demonstrate that oleocanthal abrogates fibrillization of tau by locking tau into the naturally unfolded state. Using PHF6 consisting of the amino acid residues VQIVYK, a hexapeptide within the third repeat of tau that is essential for fibrillization, we show that oleocanthal forms an adduct with the lysine via initial Schiff base formation. Structure and function studies demonstrate that the two aldehyde groups of oleocanthal are required for the inhibitory activity. These two aldehyde groups show certain specificity when titrated with free lysine and oleocanthal does not significantly affect the normal function of tau. These findings provide a potential scheme for the development of novel therapies for neurodegenerative tauopathies.

Keywords

tau; fibrillization; neurodegeneration; oleocanthal; aldehyde; lysine

Neurofibrillary tangles (NFTs), one of the two major hallmark lesions of Alzheimer's disease (AD), are comprised of tau, a microtubule (MT) associated protein (Weingarten et al. 1975; Cleveland et al. 1977; Lee et al. 1991). Multiple mechanisms including genetic mutations, posttranslational modifications, and intracellular environmental changes have been suggested to cause tau misfolding and fibrillization to form NFTs which bear the properties of amyloid deposits (Lee et al. 2001). In addition to AD, NFTs define a group of

Address correspondence and reprint requests to: Virginia M.-Y. Lee, Ph. D., the Center for Neurodegenerative Disease Research, Department of Pathology and Laboratory Medicine, Maloney 3, Hospital of the University of Pennsylvania, 3600 Spruce Street, Philadelphia, PA 19104-4283; Tel. 215 662-6427; Fax. 215 349-5909; E-mail: vmylee@mail.med.upenn.edu..

Supporting information available Supplemental data on LC-MS analysis of reaction between oleocanthal and *N*-Bz-Lys-OMe, schematic of oleocanthal modified PHF6 peptide, LC-MS analysis of reaction between oleocanthal and PHF6 peptide and spectral data for piperidine **5**.

related neurodegenerative diseases collectively known as tauopathies (Lee et al. 2001; Spillantini et al. 2006). Evidence for a direct role of tau in neurodegenerative disorders was provided when autosomal dominantly inherited tau (*MAPT*) genetic mutations were found in the group of neurodegenerative disorders collectively know as frontotemporal dementia and parkinsonism linked to chromosome 17 (FTDP-17) (Spillantini et al. 1998; Hutton et al. 1998; Poorkaj et al. 1998). To date, 39 different mutations in the tau gene from more than 100 families have been identified and tau pathology is an invariable feature of these cases (Lee et al. 2001; Goedert 2005; Goedert and Spillantini 2006). Although the exact role of tau aggregates in AD and other sporadic tauopathies is unknown, the connection between *MAPT* gene mutations and FTDP-17 suggests that the formation of tau lesions in sporadic neurodegenerative diseases may represent a final common pathway leading to neurodegeneration (Lee et al. 2001; Avila et al. 2006).

Over the last decade, a large number of tau transgenic mouse models have been established and some of these models recapitulate phenotypes found in neurodegenerative tauopathies (Lee et al. 2005). For example, age dependent formation of insoluble tau tangles, neurodegeneration and neuron loss are features of several of the models (Lee et al. 2005; Yoshiyama et al. 2007). Thus, tau misfolding and fibril assembly represents an important target for AD therapy. Indeed, a few recent reports have focused on inhibiting tau fibrillization; however no “drug-like” leads have emerged from these studies (Chirita et al. 2004; Pickhardt et al. 2005; Taniguchi et al. 2005; Necula et al. 2005; Ballatore et al. 2007).

Olive oil, the prime fat component of the Mediterranean diet, contains high levels of monounsaturated fatty acids and phytochemicals including polyphenolic compounds, squalene, and α-tocopherol (Stark and Madar 2002; Visioli and Galli 2002). These polyphenols have been implicated in defining the bitterness, pungency, and astringency of olive oil (Artajo et al. 2006). Epidemiological data suggest that olive oil has health-conferring properties that can lower risks of coronary heart disease and cancer (Giugliano and Esposito 2005; Colomer and Menendez 2006). Furthermore, several studies indicate that olive oil may delay cognitive decline (Solfrizzi et al. 1999). These health benefits have been attributed to the antioxidant constituents in olive oil. However, the exact chemical entities offering such health-promoting effects and the mechanism(s) mediating these effects, remains unknown.

In 2005, (-)-oleocanthal, the dialdehydic form of (-)-deacetoxy-ligstroside aglycone present in freshly-pressed extra virgin olive oil, and responsible for pharyngeal irritation, was discovered to hold the properties of a non-steroidal anti-inflammatory drug (NSAID) (Beauchamp et al. 2005). Shortly thereafter the synthesis and assignment of the absolute stereochemistry of the enantiomers of oleocanthal was achieved (Smith et al. 2005; Smith et al. 2007). Biological characterization established both the natural and unnatural enantiomers of oleocanthal as inhibitors of cyclooxygenases (Fig. 1b), with similar potencies as ibuprofen (Beauchamp et al. 2005). Previously, ibuprofen and the related NSAID naproxen both appear to bind plaques in the AD brain and to display anti-aggregation activities on Aβ (Agdeppa et al. 2003). Our unpublished results indicate that such an anti-aggregation activity is shared by oleocanthal. Therefore, we reasoned that oleocanthal might impede tau aggregation as well due to the common amyloidogenic nature of tau and Aβ.

Towards this end, oleocanthal was tested for inhibition of the filament formation of both the longest tau isoform T40 and the corresponding MT-binding region K18 (Fig. 1a). In both cases inhibition of tau fibrillization was observed. Given that oleocanthal contains two aldehyde groups, we speculated that tau might be covalently modified, specifically at the lysines. The studies described herein reveal that oleocanthal indeed forms an adduct with the lysine residues via initial Schiff base formation (Fig. 1c) and thereby inhibits tau

fibrillization. Additional experiments using FTIR demonstrate that oleocanthal reacts with tau in the random coil form and prevents its conversion to the β-pleated sheet conformation. Structural activity studies of a series of oleocanthal analogues suggest that both aldehyde functional groups are essential for the inhibitory activity of oleocanthal.

Materials and methods

Chemicals, peptide and synthesis of oleocanthal and oleocanthal analogues

The amyloid-binding dye thioflavine T (ThT) and α-Cyano-4-hydroxycinnamic acid (CHCA) were purchased from Sigma-Aldrich (St. Louis, MO, USA). *N*-Bz-Lys-OMe was obtained from Bachem Bioscience, Inc. (King of Prussia, PA, USA). Low molecular weight heparin sodium salt with an average MW of 5000 Da was obtained from MP Biomedicals, LLC (Aurora, OH, USA). N- and C-terminal protected PHF6 tau peptide, i.e., Ac-VQIVYK-amide, was purchased from W. M. Keck Biotechnology Resource Center (New Haven, CT, USA). Oleocanthal and oleocanthal analogues were synthesized as described (Smith et al. 2005; Smith et al. 2007).

Cloning, expression and purification of proteins

The longest wild type (WT) human tau isoform T40 (441 amino acid residues) and the tau K18 constructs consisting of the four-repeat MT binding region (Q244-E372, amino acids numbered as in T40) (Fig. 1a) were generated as described (Li and Lee 2006). For molecular cloning, the PCR product was inserted between the Nde I and EcoR I sites of the bacterial expression vector pRK172. Minipreps of the subcloned DNA plasmids were sequenced and verified. The proteins were expressed in *Escherichia coli* BL21(DE3) RIL and purified as described (Li and Lee 2006).

Filament assembly and oleocanthal inhibition experiment

For tau filament assembly, 20 μM protein in 100 mM sodium acetate, pH 7.0 was agitated in thin-wall PCR tubes at 37 °C at 1000 rpm in the presence of 2 mM DTT, 0.04% sodium azide and 50 μM low-molecular-weight heparin. When oleocanthal or related analogues were tested for inhibition of tau fibrillization, the reaction was incubated without agitation. Oleocanthal and the analogues (0-100 μM in 5% DMSO v/v) were added to the reaction mixture, and the same percentage of DMSO was used for controls. ThT fluorescence assay, sedimentation analysis and negative staining electron microscopy (EM) were conducted as described to monitor the fibrillization process and examine the morphology of the fibrils formed (Li and Lee 2006). Experiments were repeated with at least two preparations of purified proteins for at least 3 times.

To determine the IC50 of oleocanthal, heparin induced tau fibrillization was performed as described (Crowe et al. 2007) with the following changes: the tau fragment used was K18 containing the P301L missense mutation (K18PL) which fibrillizes faster than the wild type K18. Briefly, 15 μL of 33.3 μM K18PL was pipetted into a 384-well plate. Compound was added using a Perkin Elmer Evolution P3 dispenser with the pin tool (100 nL volume) to yield the desired compound concentration, followed by addition of 10 μL of 50 μM heparin to yield a final fibrillization reaction mixture of 20 μM tau and 20uM heparin. The mixture was incubated for 6 hrs at 37 °C and the fibrillization was measured by ThT fluorescence. In essence, 25 μL of 25 μM ThT in 100 mM glycine, pH 8.5 was added to the fibrillization reaction to yield a final ThT concentration of 12.5 μM and incubated for 1 hr at room temperature. Fluorescence was read at excitation 450 nm emission 510 nm and compound efficacy was plotted as percent inhibition of fibrillization as compared to DMSO controls. To evaluate the specificity of oleocanthal in reacting with the amino group of lysine, a final

concentration of 0.158 μM to 1 mM lysine was added to the fibrillization experiment described above.

Mass spectrometric analysis of K18 after incubation with oleocanthal

20 μM peptide was incubated with or without 100 μM oleocanthal in 10 mM NaOAc buffer, pH 7.0 at 37 °C for 8 hrs. Samples were mixed with equal volume of 100 mM ammonium bicarbonate buffer, pH 7.7 to quench the remaining free aldehyde groups of oleocanthal. After a five-fold dilution with deionized water, 1 μL was spotted onto the gold MALDI target plate and allowed to dry before analysis by MALDI-TOF MS. Protein molecular ions were analyzed in linear, positive ion mode using a Voyager Elite mass spectrometer (Applied Biosystems, Foster City, CA, USA). The settings of the mass spectrometer were as follows: Acceleration voltage 25 kV; Grid voltage 99%; Guide wire 0.2%; Extraction delay time 800 nsec; Laser intensity 2200 V. Each spot was analyzed a minimum of three times, accumulating spectra composed of approximately 150 shots in total.

Mass spectrometric analysis of PHF6 (Ac-VQIVYK-amide) peptide and N-Bz-Lys-OMe after incubation with oleocanthal

Liquid chromatography-mass spectrometry (LC-MS; Waters) analysis was performed using reverse phase (acetonitrile:water) chromatography. Detection methods for this instrument include light scattering (ELS), photodiode array (PDA), and mass spectrometry (ESI and APCI in positive and negative modes).

Samples were prepared by mixing equimolar amounts of oleocanthal and PHF6 peptide or *N*-Bz-Lys-OMe in either methanol or pH 7 phosphate buffer to about 0.05 M. After 8 hrs at 23 °C, the crude reaction mixtures were diluted with a 1:1 acetonitrile:water mixture for analysis. For reductions, the methanolic solutions were first cooled to 0 °C and two molar equivalents of sodium borohydride was added. After 30 min at this temperature and 30 min at room temp, the reaction was quenched with water and diluted with an equal volume of acetonitrile for analysis.

Infrared spectroscopy

The samples for infrared spectroscopy were prepared as described (von Bergen et al. 2000). Polarized attenuated total internal reflection Fourier transform infrared (PATIR-FTIR) spectra were collected in rapid-scanning mode as 1024 co-added interferograms using a Bio-Rad FTS-60A spectrometer, a liquid-nitrogen cooled MCT detector, a resolution of 2 cm^{-1}, scanning speed of 20 MHz, and an undersampling ratio of 2. Atmospheric water vapor was removed by flushing the spectrometer with dry air. After a reference spectrum of the instrument was recorded, 10 μL of 10 mg/mL tau protein in D_2O was applied onto a germanium internal reflection crystal by evaporation, and the absorbance spectrum of the sample was measured. Spectra were processed with one level of zero filling and triangular apodization, but no smoothing, deconvolution, vapor subtraction, or non-level baseline correction. To facilitate comparison, the spectra were normalized with respect to their maxima. IR spectra were fit by using Origin 6.1 software (OriginLab, Northampton, MA). Each spectrum was fit with one straight and level baseline and multi Lorentzian bands. Each band was specified by frequency, and full width at half-maximum (FWHM).

Microtubule assembly assay

Microtubule (MT) assembly was measured by turbidity at 350 nm in 384-well plates and was adapted from a published study (Hong et al. 1998). Briefly, compounds were incubated at room temperature at 50 μM in the presence of tau in RAB buffer [100 mM MES, 1 mM EGTA and 0.5 mM $MgSO_4$, pH 6.9]. Ice cold tubulin (Cytoskeleton, Denver, CO, USA)

was dispensed into a pre-cooled plate followed sequentially by GTP, then by the tau/compound mixture to yield a final volume of 50 μL with a concentration of 30 μM tubulin, 1 mM GTP, and 15 μM T40. This dilution resulted in a compound concentration of 46 μM during the MT assembly assay. The plate was then immediately incubated in a Spectramax M5 plate reader at 37 °C and the turbidity measured every 60 seconds. Each assay was done in triplicate and compared to triplicate DMSO controls.

Results

Oleocanthal inhibits K18 fibrillization

The ability of oleocanthal to inhibit tau fibrillization was assayed at 0 μM, 1 μM, 10 μM and 100 μM. The fibrillization reaction was probed with ThT, a fluorescent dye specific for the detection of β-pleated sheet structures. Oleocanthal significantly reduced the fibrillization of 20 μM K18 compared with the control (Fig. 2a). Even at 1 μM oleocanthal, ~ 60% inhibition of K18 fibril assembly was observed in our ThT assay. At 10 μM oleocanthal, the inhibition increased to ~70%, and when the concentration of oleocanthal reached 100 μM, the ThT reading remained at background level throughout the experiment. To confirm that the ThT result indeed reflects the inhibition of K18 fibrillization by oleocanthal, sedimentation analyses were conducted (Fig. 2b). Although oleocanthal appeared less potent based on the sedimentation assay (probably due to the inability of ThT in detecting all tau aggregates), the general trend of inhibition correlated well with the ThT assay. The inhibitory effect of oleocanthal on K18 fibrillogenesis was further verified by EM (Fig. 2c). At 10 μM oleocanthal, almost all of the structures visualized on the grids were either short filaments or globular structures, suggesting that the elongation step of tau polymerization was disrupted. Meanwhile, samples containing K18 incubated with 100 μM oleocanthal were totally devoid of any filaments or nascent fibrils. With a fast fibrillizing K18 mutant, K18PL, the IC50s of (-) natural and (+) unnatural oleocanthal were determined to be approximately 2.9 and 3.5 μM, respectively (Fig. S1).

Oleocanthal inhibits T40 fibrillization

The ability of oleocanthal to inhibit tau fibrillization extended to the full-length tau protein T40. In this experiment, the concentration of T40 was maintained at the same level as that of K18 (i.e., 20 μM). Since T40 fibrillizes much slower than K18, the incubation time was increased from 24 hrs to 15 days. Though less potent than in the K18 experiment, oleocanthal remained inhibitory for the fibrillization of T40. At 1 μM, oleocanthal exhibited modest inhibitory activity towards T40 compared with K18, whereas significant inhibition (50%) was observed with 10 μM oleocanthal at the end of the assay. At 100 μM oleocanthal, complete inhibition of T40 fibrillization was observed (Fig. 3a) similar to that for K18. The inhibitory effects of oleocanthal on T40 were confirmed by both semi-quantitative sedimentation analysis (Fig. 3b) and EM studies (Fig. 3c), wherein inhibition was essentially complete with 100 μM oleocanthal.

Tau modification and possible crosslinking by oleocanthal

To determine if oleocanthal inhibits tau fibrillization via covalent bonding, we explored the possibility that the two aldehydes and the alkene react with certain amino acid residues in tau. Such reactivity could involve: (A) imine formation between the aldehyde and the ε-amino group of lysine; (B) Michael addition between the alkene group and the thiol group of cysteine, and/or (C) imine formation or Michael addition between with the imidazole nitrogen of histidine. There are 19 Lys, 2 Cys and 12 His residues in K18 and 44 Lys, 2 Cys and 5 His in T40. Depending on the reactivity of the peptide/protein functional groups, crosslinking might occur. To address this question, 20 μM K18 was incubated with 100 μM oleocanthal at 37 °C for 8 or 24 hrs; the samples were then resolved on a 15% SDS-PAGE

gel. High molecular weight products were detected after Coomassie staining, suggesting that oleocanthal modifies and crosslinks tau by covalent modification (Fig. 4a). The size of the bands corresponds to K18 monomer, dimer, trimer, tetramer, etc. SDS-PAGE analysis of 20 μM T40 incubated with 0, 1, 10 and 100 μM oleocanthal also revealed crosslinked tau bands (Fig. 4b).

The aforementioned 8-hr oleocanthal modified K18 samples were also analyzed by mass spectrometry (MALDI). Although the spectra are noisy, which prohibits accurate definition of the exact masses and hence stoichiometry analysis, it is clear that the population of masses expands towards higher Mr after reaction. Detailed analysis of the data is also complicated by the potential crossinking of oleocanthal. This provides further evidence that oleocanthal modifies and possibly crosslinks tau (Fig. 4c).

Oleocanthal inhibits the polymerization of PHF6 peptide through modification of the lysine residue

Since PHF6, the hexapeptide VQIVYK in the third MT binding repeat of tau, is required for the formation of tau fibrils (Li and Lee 2006), and given that this peptide contains a single Lys at the C-terminus, we reasoned that oleocanthal might inhibit PHF6 fibrillization. To investigate this possibility, we first demonstrated that PHF6 forms fibrils similar to those formed by full-length tau as revealed by negative staining EM (Fig. 5a). Then we examined the kinetics of PHF6 fibril formation upon inhibition by oleocanthal through monitoring the fluorescence signal produced by ThT, when bound to the polymerized peptide (Goux et al. 2004). The inhibition, which was dose dependent (Fig. 5b), appears as both decreased rate of PHF6 polymerization and decreased maximum ThT reading (Table 1).

The inhibition of PHF6 fibrillization upon treatment with oleocanthal could be due to either covalent modification or noncovalent association. To elucidate this interaction between oleocanthal and PHF6, we first conducted a model study with a lysine derivative, *N*-Bz-Lys-OMe (Fig. 5c). Incubation of *N*-Bz-Lys-OMe with oleocanthal in methanol followed by LC-MS analysis of the reaction mixture revealed a mass of 551 (Fig. 5d and Fig. S2) corresponding to the formation of a Schiff base adduct **2** $[M+H]^+$. NMR analysis of the same sample, however, failed to detect the α,β-unsaturated aldehyde, suggesting that cyclization of the imine nitrogen with the unsaturated aldehyde carbonyl had occurred. A mass at 533 (i.e. **4**) corresponding to the loss of H_2O and is consistent with the proposed cyclization. After reduction with sodium borohydride, LC-MS analysis revealed a mass at 537 (i.e., loss of 14 amu from the initial adduct) (Fig. 5e and Fig. S3) that presumably arises through the addition of two hydrogens and the loss of an oxygen as seen in **5**. The second largest peak at 523 is consistent with the mass of $[MOCH_3]^+$, corresponding to the expected loss of the lysine methoxy group. Given that 1,5-dialdehydes are well known precursors of functionalized piperidines upon condensation with primary amines, followed by sodium borohydride reduction (Hanessian et al. 1990), we envision a similar process takes place here. Further support for this reaction sequence was provided by the isolation and structure confirmation of piperidine **5** (Supplemental Data).

To demonstrate a similar covalent modification of the PHF6 peptide by oleocanthal, we repeated the same experiment, incubating oleocanthal with the peptide (Fig. 5f and Fig. S4). Before reduction, LC-MS revealed the presence of masses at 1077 $[M+H]^+$, as well as 1059 $[M+H-H_2O]^+$ (Fig. 5g and Fig. S5), the former corresponding to Schiff base formation between the lysine residue and oleocanthal (**6** or **7**), the latter to the loss of H_2O consistent with cyclization (**8**). Sodium borohydride reduction led to an observed mass at 1063 (Fig. 5h and Fig. S6), again consistent with piperidine ring formation (**9**) as observed in the model system described above. The same peak was observed when the solvent was changed from methanol to 100 mM (pH 7) phosphate buffer (Fig. S7). Taken together, these results clearly

indicate that oleocanthal can covalently modify PHF6 at the lysine residue. However, oleocanthal may react with other lysine residues as well.

Oleocanthal prevents random coil to β-sheet conformational change of tau

To determine how covalent modification of tau by oleocanthal prevents fibril formation, we employed FTIR to monitor the secondary structure of tau in the presence or absence of oleocanthal. Tau normally does not possess significant secondary structures, but upon fibrilization undergoes transition from random coil to increased β-sheet content (von Bergen et al. 2001; Barghorn and Mandelkow 2002). To elucidate whether oleocanthal inhibits tau fibrillization by preventing this conformational change, we incubated K18 and T40 with or without oleocanthal at a molar ratio of 2:1 (protein/compound). As expected, in the absence of oleocanthal, K18 fibrillization occurred accompanied with an increase in β-pleated sheet structure indicated by a maximum intensity occurring at ~1629 wavenumbers (Fig. 6a). In contrast, in the presence of oleocanthal, a shift in the maximum intensity (at ~1636 wavenumbers) was not observed, with the spectrum remaining the same as that of the K18 sample before fibrillization. Deconvolution analysis yielded an estimate of ~ 60% β-sheet for fibrillized K18 but no β-sheet for the other samples. These results suggest that oleocanthal keeps K18 mostly in random coil. A similar comparison was observed with the FTIR spectra of T40 alone or when incubated with oleocanthal (Fig. 6b). The absorbance maximum for oleocanthal treated T40 remained at ~1640 wavenumbers, a signature of random coil, while the spectrum for untreated T40 maximized at ~1632 wavenumbers, suggesting the emergence of β-pleated sheet structures. The β-sheet content of untreated T40 was estimated to be ~57% after 17d assembly while those of the rest samples were hardly revealed through deconvolution analysis. Thus, oleocanthal appears to inhibit tau fibrillization by arresting the conversion of tau from random coil to β-sheet conformation via covalent modification.

Definition of the structure in oleocanthal responsible for inhibition of tau fibrillization

To define the pharmacophore in oleocanthal required for inhibition of tau fibrillization, we performed a structure activity relationship (SAR) study involving the design, synthesis (Smith et al. 2007) and evaluation of analogues **10**-**25** (Fig. 7a). Analogues **10**-**16**, **18**, **21**, and **22**, wherein the phenolic moiety was systematically varied, displayed the same level of activity as oleocanthal (Fig. 7b and 7c). Particularly striking is the identical activity of the diminutive analogue methyl ester **11** to oleocanthal (**1**), suggesting that the anti-fibrillization pharmacophore comprises both the saturated and unsaturated aldehyde moieties. Indeed, diols **17** (the immediate synthetic precursor to oleocanthal) and **19**, both lacking the two aldehyde functionalities, showed no inhibitory activity towards tau fibrillization. This was anticipated in light of the previous observation that oleocanthal initially forms a Schiff base with lysine residues in tau. Anomaly in the dialdehyde series of analogues was observed for the saturated dialdehyde **23**, lacking the olefin. However, during the course of experiments, we discovered that **23**, like many saturated 1, 5-dialdehydes (Parks et al. 2006), decomposes under the assay conditions after approximately 6 hrs. We next examined a series of monoaldehyde analogues, **20**, **24** and **25**. When either of the aldehyde carbonyls was reduced, a significant loss in activity was observed. It should be noted that analogues **24** and **25** exist in the thermodynamically more stable lactol forms, which are in equilibrium with their respective hydroxy aldehyde forms. Taken together, these SAR studies clearly indicate that the two aldehyde groups present in oleocanthal are essential to prevent tau fibrillogenesis. Interestingly, these two aldehyde groups of oleocanthal show certain selectivity as evidenced by our lysine titration experiment (Fig. 8). In this experiment, significant reduction of the inhibitory activity of oleocanthal was not observed until the concentration of free lysine reached millimolar range.

Oleocanthal does not significantly affect the ability of tau to promote MT assembly

The microtubule binding region of tau also comprises the core sequence for tau aggregation. Our unpublished results suggest a general correlation between the ability of tau to promote microtubule assembly and the tendency for tau to form paired helical filaments. Hence, tau aggregation inhibitors might compromise the physiological function of tau to stabilize MTs. Therefore, the effect of oleocanthal on tau-induced MT assembly was evaluated in comparison with methylene blue, a tau aggregation inhibitor reported to be effective in arresting the progression of AD in clinical trials (Wischik et al. 2008). Briefly, 15 μM T40 was pre-incubated with 50 μM compounds in RAB buffer and then the mixture was added to 30 μM tubulin to induce MT assembly. Although both compounds seemed to reduce the polymerization of tubulin, the changes were not statistically significant (Fig. S8). Such behavior has been shown for methylene blue and several other tau aggregation inhibitors previously (Pickhardt et al. 2005; Taniguchi et al. 2005). Our data suggest that oleocanthal does not significantly interfere with tau-microtubule interaction.

Discussion

High consumption of extra virgin olive oil in the Mediterranean region has long been associated with lower occurrences of certain chronic diseases, such as cancer and cardiovascular ailments(Giugliano and Esposito 2005; Colomer and Menendez 2006), as well as a reduced risk of AD or related neurodegenerative dementias (Solfrizzi et al. 1999; Solfrizzi et al. 2003; Panza et al. 2004; Solfrizzi et al. 2005; Wischik et al. 2008). These health benefits are usually attributed to the antioxidative function of monounsaturated lipids, such as oleic acid. Minor phenolic compounds found in extra virgin olive oil have also been shown to bear antioxidant, anti-inflammatory and anti-thrombic activities (Baldioli et al. 1996; Owen et al. 2000a; Owen et al. 2000b; Manna et al. 2002), although the exact mechanism of action remains unknown.

Oleocanthal, the principal pharyngeal irritant in extra virgin olive oil usually comprises about 0.02% by weight (Impellizzeri and Lin 2006). Since it only represents about 10% of the total phenolic compounds (Fogliano and Sacchi 2006), the other phenolic compounds may also contribute to the neuroprotective activities of olive oil. The discovery that oleocanthal is a potent non-steroidal anti-inflammatory agent similar in potency to ibuprofen opened new avenues for the possible beneficial effects of olive oil (Beauchamp et al. 2005), since ibuprofen and a related subset of NSAIDs have recently been shown to both lower amyloidogenic Aβ42 levels (Zhou et al. 2003), and alter β-amyloid processing and deposition in an animal model of AD (Yan et al. 2003), via activities independent of their effects on cyclooxygenase. Additional studies have revealed that NSAIDS, including aspirin, ibuprofen and naproxen, inhibit Aβ aggregation *in vitro* (Thomas et al. 2001), suggesting yet another mechanism. These reports point to a possible link between the health benefits of NSAID components in olive oil and the pathogenesis of AD. Preliminary data from our laboratories also suggests that oleocanthal inhibits the fibrillization of both Aβ40 and Aβ42 *in vitro* (unpublished results). The similarities between the amyloidgenic proteins Aβ and tau in forming β-sheet strands further suggest a common mechanism of fibril formation and thus prompted us to explore oleocanthal as a potential inhibitor for tau fibrillization. Interestingly, although we demonstrated here that oleocanthal is effective in inhibiting tau assembly into paired helical filaments, other NSAIDs, including aspirin, ibuprofen, naproxen flurbiprofen, indomethacin failed to block tau fibrillization at concentration up to 100 μM (data not shown). Thus, the inhibitory effect of oleocanthal on tau fibril formation represents a novel activity not shared by other NSAIDs.

To gain insights into the mechanism(s) of this inhibition, we find that oleocanthal forms an adduct with the lysine residue in the PHF6 peptide (corresponding to K311 in tau protein,

which is a critical site for tau fibrillization) (Li and Lee 2006). We have previously reported on the importance of K311 residue and shown that when it is removed or mutated to aspartate, tau loses the ability to form filaments. Modification of this site by oleocanthal can yield either a neutral or negatively charged residue should the ester bond of oleocanthal hydrolyzes. If hydrolysis does occur, the effect of the modification may well mimic a K→D substitution. This charge manipulation and/or the introduction of steric hindrance would be expected to alter the local conformation of the PHF6 motif and thereby disrupt tau-tau interaction, which is essential for β-sheet structure development and eventual fibril formation. Although the present study did not directly answer whether other lysine residues are modified by oleocanthal, crosslinking of tau was detected by SDS-PAGE suggesting that reaction with the aldehyde groups of oleocanthal could occur at multiple lysine residues. Such modifications probably lead to the inhibition of tau filament assembly as well. However, addition of nearly millimolar range of free lysine in tau aggregation failed to suppress the inhibitory action of oleocanthal. This provides at least indirect evidence that the aldehyde groups of oleocanthal might bear some selectivity.

The α,β-unsaturated aldehyde of oleocanthal is a functional group shared by acrolein. Studies, however, have shown that acrolein does not affect tau fibrillization at 10 μM, a concentration sufficient for near complete inhibition by oleocanthal. At higher concentrations (i.e., 1 mM), acrolein does inhibit tau fibrillization (data not shown). The higher potency of oleocanthal compared to acrolein is consistent with our SAR observations suggesting that initial Schiff base formation occurs at the more reactive saturated aldehyde. The same SAR study also suggests that the unsaturated aldehyde group is required to avoid the presumed cyclization reaction in the analogues **24** and **25**. Not surprisingly, oleocanthal analogue (−)-**14**, which is also found in olive oil and bears the same dialdehyde pharmacophore, is another potent inhibitor of tau fibrilization. Such compounds may have additive or synergistic effects on other related physiological functions as well, such as LDL oxidation and blood pressure (Fogliano and Sacchi 2006).

In summary, we present evidence that oleocanthal inhibits tau aggregation *in vitro* and such inhibition shows high potency and some selectivity. *In vivo* studies using relevant cell and animal models are warranted to further evaluate the efficacy and toxicity of oleocanthal. Meanwhile, oleocanthal might have other neuroprotective benefits due to the non-steroidal anti-inflammatory and anti-oxidant activities. Therefore, oleocanthal might hold potential as a lead compound for the development of small molecule inhibitors of amyloidogenesis in neurodegenerative diseases.

Supplementary Material

Refer to Web version on PubMed Central for supplementary material.

Acknowledgments

We thank Chi Li for technical support on molecular cloning and the Biochemical Imaging Core Facility of the University of Pennsylvania for assistance in the EM studies. We gratefully acknowledge Dr. Michael Myers for his help with LC-MS analyses, William DeGrado for providing access for the MALDI instrument, Dr. Liu Liu for his assistance with the analysis of IR spectra. We also appreciate the helpful discussions from Dr. Paul Axelsen, Dr. Carlo Ballatore, Dr. Ian Murray and Dr. William DeGrado. The study is supported by NIH grants AG17586. V. M.-Y. L. is the John H. Ware III Professor for Alzheimer's Research.

Abbreviations used

The abbreviations used are:

Aβ	amyloid β peptide
AD	Alzheimer's disease
CHCA	α-Cyano-4-hydroxycinnamic acid
EM	electron microscopy
FTDP-17	frontotemporal dementia and parkinsonism linked to chromosome 17
MALDI-TOF	matrix-assisted laser desorption/ionization-time of flight
NFTs	neurofibrillary tangles
NSAID	non-steroidal anti-inflammatory drug
PATIR-FTIR	polarized attenuated total internal reflection Fourier transform infrared
PMSF	phenylmethylsulfonyl fluoride
SAR	structure-activity relationship
SDS-PAGE	sodium dodecyl sulphate polyacrylamide gel electrophoresis
ThT	thioflavine T

References

Agdeppa ED, Kepe V, Petric A, Satyamurthy N, Liu J, Huang SC, Small GW, Cole GM, Barrio JR. In vitro detection of (S)-naproxen and ibuprofen binding to plaques in the Alzheimer's brain using the positron emission tomography molecular imaging probe 2-(1-{6-[(2[F-18]fluoroethyl)(methyl)amino]-2-naphthyl}ethylidene) malononitrile. Neuroscience. 2003; 117:723–730. [PubMed: 12617976]

Artajo LS, Romero MP, Morello JR, Motilva MJ. Enrichment of refined olive oil with phenolic compounds: Evaluation of their antioxidant activity and their effect on the bitter index. J. Agric. Food Chem. 2006; 54:6079–6088. [PubMed: 16881720]

Avila J, Santa-Maria I, Perez M, Hernandez F, Moreno F. Tau phosphorylation, aggregation, and cell toxicity. J. Biomed. Biotechnol. 2006; 2006:74539. [PubMed: 17047313]

Baldioli M, Servili M, Perretti G, Montedoro GF. Antioxidant activity of tocopherols and phenolic compounds of virgin olive oil. J. Am. Oil Chem. Soc. 1996; 73:1589–1593.

Ballatore C, Lee VM-Y, Trojanowski JQ. Tau-mediated neurodegeneration in Alzheimer's disease and related disorders. Nat. Rev. Neurosci. 2007; 8:663–672. [PubMed: 17684513]

Barghorn S, Mandelkow E. Toward a unified scheme for the aggregation of tau into Alzheimer paired helical filaments. Biochemistry. 2002; 41:14885–14896. [PubMed: 12475237]

Beauchamp GK, Keast RSJ, Morel D, Lin JM, Pika J, Han Q, Lee CH, Smith AB, Breslin PAS. Phytochemistry - Ibuprofen-like activity in extra-virgin olive oil. Nature. 2005; 437:45–46. [PubMed: 16136122]

Chirita C, Necula M, Kuret J. Ligand-dependent inhibition and reversal of tau filament formation. Biochemistry. 2004; 43:2879–2887. [PubMed: 15005623]

Cleveland DW, Hwo SY, Kirschner MW. Purification of Tau, A Microtubule-Associated Protein That Induces Assembly of Microtubules from Purified Tubulin. J. Mol. Biol. 1977; 116:207–225. [PubMed: 599557]

Colomer R, Menendez JA. Mediterranean diet, olive oil and cancer. Clin. Transl. Oncol. 2006; 8:15–21. [PubMed: 16632435]

Crowe A, Ballatore C, Hyde E, Trojanowski JQ, Lee VM-Y. High throughput screening for small molecule inhibitors of heparin-induced tau fibril formation. Biochem. Biophys. Res. Commun. 2007; 358:1–6. [PubMed: 17482143]

Fogliano V, Sacchi R. Oleocanthal in olive oil: Between myth and reality. Mol. Nutr. Food Res. 2006; 50:5–6. [PubMed: 16397870]

Giugliano D, Esposito K. Mediterranean diet and cardiovascular health. Ann. N. Y. Acad. Sci. 2005; 1056:253–260. [PubMed: 16387693]

Goedert M. Tau gene mutations and their effects. Mov. Disord. 2005; 20:S45–S52. [PubMed: 16092090]

Goedert M, Spillantini MG. A century of Alzheimer's disease. Science. 2006; 314:777–781. [PubMed: 17082447]

Goux WJ, Kopplin L, Nguyen AD, Leak K, Rutkofsky M, Shanmuganandam VD, Sharma D, Inouye H, Kirschner DA. The formation of straight and twisted filaments from short tau peptides. J. Biol. Chem. 2004; 279:26868–26875. [PubMed: 15100221]

Hanessian S, Faucher AM, Leger S. Total Synthesis of (+)-Meroquinene. Tetrahedron. 1990; 46:231–243.

Hong M, Zhukareva V, Vogelsberg-Ragaglia V, Wszolek Z, Reed L, Miller BI, Geschwind DH, Bird TD, McKeel D, Goate A, Morris JC, Wilhelmsen KC, Schellenberg GD, Trojanowski JQ, Lee VM-Y. Mutation-specific functional impairments in distinct Tau isoforms of hereditary FTDP-17. Science. 1998; 282:1914–1917. [PubMed: 9836646]

Hutton M, Lendon CL, Rizzu P, Baker M, Froelich S, Houlden H, Pickering-Brown S, Chakraverty S, Isaacs A, Grover A, Hackett J, Adamson J, Lincoln S, Dickson D, Davies P, Petersen RC, Stevens M, de Graaff E, Wauters E, van Baren J, Hillebrand M, Joosse M, Kwon JM, Nowotny P, Che LK, Norton J, Morris JC, Reed LA, Trojanowski J, Basun H, Lannfelt L, Neystat M, Fahn S, Dark F, Tannenberg T, Dodd PR, Hayward N, Kwok JBJ, Schofield PR, Andreadis A, Snowden J, Craufurd D, Neary D, Owen F, Oostra BA, Hardy J, Goate A, van Swieten J, Mann D, Lynch T, Heutink P. Association of missense and 5'-splice-site mutations in tau with the inherited dementia FTDP-17. Nature. 1998; 393:702–705. [PubMed: 9641683]

Impellizzeri J, Lin JM. A simple high-performance liquid chromatography method for the determination of throat-burning oleocanthal with probated antiinflammatory activity in extra virgin olive oils. J. Agric. Food Chem. 2006; 54:3204–3208. [PubMed: 16637673]

Lee VM-Y, Goedert M, Trojanowski JQ. Neurodegenerative tauopathies. Annu. Rev. Neurosci. 2001; 24:1121–1159. [PubMed: 11520930]

Lee VM-Y, Balin BJ, Otvos L, Trojanowski JQ. A68 - A Major Subunit of Paired Helical Filaments and Derivatized Forms of Normal-Tau. Science. 1991; 251:675–678. [PubMed: 1899488]

Lee VM-Y, Kenyon TK, Trojanowski JQ. Transgenic animal models of tauopathies. Biochim. Biophys. Acta. 2005; 1739:251–259. [PubMed: 15615643]

Li W, Lee VM-Y. Characterization of two VQIXXK motifs for tau fibrillization in vitro. Biochemistry. 2006; 45:15692–15701. [PubMed: 17176091]

Manna C, D'Angelo S, Migliardi V, Loffredi E, Mazzoni O, Morrica P, Galletti P, Zappia V. Protective effect of the phenolic fraction from virgin olive oils against oxidative stress in human cells. J. Agric. Food Chem. 2002; 50:6521–6526. [PubMed: 12381144]

Necula M, Chirita CN, Kuret J. Cyanine dye N744 inhibits tau fibrillization by blocking filament extension: Implications for the treatment of tauopathic neurodegenerative diseases. Biochemistry. 2005; 44:10227–10237. [PubMed: 16042400]

Owen RW, Giacosa A, Hull WE, Haubner R, Spiegelhalder B, Bartsch H. The antioxidant/anticancer potential of phenolic compounds isolated from olive oil. Eur. J. Cancer. 2000a; 36:1235–1247. [PubMed: 10882862]

Owen RW, Mier W, Giacosa A, Hull WE, Spiegelhalder B, Bartsch H. Phenolic compounds and squalene in olive oils: the concentration and antioxidant potential of total phenols, simple phenols, secoiridoids, lignans and squalene. Food Chem. Toxicol. 2000b; 38:647–659. [PubMed: 10908812]

Panza F, Solfrizzi V, Colacicco AM, D'introno A, Capurso C, Torres F, Del Parigi A, Capurso S, Capurso A. Mediterranean diet and cognitive decline. Public Health Nutr. 2004; 7:959–963. [PubMed: 15482625]

Parks BW, Gilbertson RD, Domaille DW, Hutchison JE. Convenient synthesis of 6,6-bicyclic malonamides: A new class of conformationally preorganized ligands for f-block ion binding. J. Org. Chem. 2006; 71:9622–9627. [PubMed: 17168578]

Pickhardt M, Gazova Z, von Bergen M, Khlistunova I, Wang YP, Hascher A, Mandelkow EM, Biernat J, Mandelkow E. Anthraquinones inhibit tau aggregation and dissolve Alzheimer's paired helical filaments in vitro and in cells. J. Biol. Chem. 2005; 280:3628–3635. [PubMed: 15525637]

Poorkaj P, Bird TD, Wijsman E, Nemens E, Garruto RM, Anderson L, Andreadis A, Wiederholt WC, Raskind M, Schellenberg GD. Tau is a candidate gene for chromosome 17 frontotemporal dementia. Ann. Neurol. 1998; 43:815–825. [PubMed: 9629852]

Smith AB, Han Q, Breslin PAS, Beauchamp GK. Synthesis and assignment of absolute configuration of (-)-oleocanthal: A potent, naturally occurring non-steroidal anti-inflammatory and anti-oxidant agent derived from extra virgin olive oils. Org. Lett. 2005; 7:5075–5078. [PubMed: 16235961]

Smith AB, Sperry JB, Han Q. Syntheses of (-)-oleocanthal, a natural NSAID found in extra virgin olive oil, the (-)-deacetoxy-oleuropein aglycone, and related analogues. J. Org. Chem. 2007; 72:6891–6900. [PubMed: 17685574]

Solfrizzi V, D'introno A, Colacicco AM, Capurso C, Del Parigi A, Capurso S, Gadaleta A, Capurso A, Panza F. Dietary fatty acids intake: possible role in cognitive decline and dementia. Exp. Gerontol. 2005; 40:257–270. [PubMed: 15820606]

Solfrizzi V, Panza F, Capurso A. The role of diet in cognitive decline. J. Neural Transm. 2003; 110:95–110. [PubMed: 12541015]

Solfrizzi V, Panza F, Torres F, Mastroianni F, Del Parigi A, Venezia A, Capurso A. High monounsaturated fatty acids intake protects against age-related cognitive decline. Neurology. 1999; 52:1563–1569. [PubMed: 10331679]

Spillantini MG, Murrell JR, Goedert M, Farlow M, Klug A, Ghetti B. Mutations in the tau gene (MAPT) in FTDP-17: the family with Multiple System Tauopathy with Presenile Dementia (MSTD). J. Alzheimer's Dis. 2006; 9:373–380. [PubMed: 16914875]

Spillantini MG, Murrell JR, Goedert M, Farlow MR, Klug A, Ghetti B. Mutation in the tau gene in familial multiple system tauopathy with presenile dementia. Proc. Natl. Acad. Sci. U. S. A. 1998; 95:7737–7741. [PubMed: 9636220]

Stark AH, Madar Z. Olive oil as a functional food: Epidemiology and nutritional approaches. Nutr. Rev. 2002; 60:170–176. [PubMed: 12078915]

Taniguchi S, Suzuki N, Masuda M, Hisanaga S, Iwatsubo T, Goedert M, Hasegawa M. Inhibition of heparin-induced tau filament formation by phenothiazines, polyphenols, and porphyrins. J. Biol. Chem. 2005; 280:7614–7623. [PubMed: 15611092]

Thomas T, Nadackal TG, Thomas K. Aspirin and non-steroidal anti-inflammatory drugs inhibit amyloid-beta aggregation. Neuroreport. 2001; 12:3263–3267. [PubMed: 11711868]

Visioli F, Galli C. Biological properties of olive oil phytochemicals. Crit. Rev. Food Sci. Nutr. 2002; 42:209–221. [PubMed: 12058980]

von Bergen M, Barghorn S, Li L, Marx A, Biernat J, Mandelkow EM, Mandelkow E. Mutations of tau protein in frontotemporal dementia promote aggregation of paired helical filaments by enhancing local beta-structure. J. Biol. Chem. 2001; 276:48165–48174. [PubMed: 11606569]

von Bergen M, Friedhoff P, Biernat J, Heberle J, Mandelkow EM, Mandelkow E. Assembly of tau protein into Alzheimer paired helical filaments depends on a local sequence motif ((306)VQIVYK(311)) forming beta structure. Proc. Natl. Acad. Sci. U. S. A. 2000; 97:5129–5134. [PubMed: 10805776]

Weingarten MD, Lockwood AH, Hwo SY, Kirschner MW. A protein factor essential for microtubule assembly. Proc. Natl. Acad. Sci. U. S. A. 1975; 72:1858–1862. [PubMed: 1057175]

Wischik, CM.; Bentham, P.; Wischik, DJ.; Seng, KM. Tau aggregation inhibitor (TAI) therapy with rember TM arrests disease progression in mild and moderate Alzheimer's disease over 50 weeks. Alzheimer's Association International Conference on Alzheimer's Disease; Chicago, Illinois, USA. 2008.

Yan Q, Zhang JH, Liu HT, Babu-Khan S, Vassar R, Biere AL, Citron M, Landreth G. Anti-inflammatory drug therapy alters beta-amyloid processing and deposition in an animal model of Alzheimer's disease. J. Neurosci. 2003; 23:7504–7509. [PubMed: 12930788]

Yoshiyama Y, Higuchi M, Zhang B, Huang SM, Iwata N, Saido TC, Maeda J, Suhara T, Trojanowski JQ, Lee VM-Y. Synapse loss and microglial activation precede tangles in a P301S tauopathy mouse model. Neuron. 2007; 53:337–351. [PubMed: 17270732]

Zhou Y, Su Y, Li BL, Liu F, Ryder JW, Wu X, Gonzalez-DeWhitt PA, Gelfanova V, Hale JE, May PC, Paul SM, Ni BH. Nonsteroidal anti-inflammatory drugs can lower amyloidogenic Aβ(42) by inhibiting Rho. Science. 2003; 302:1215–1217. [PubMed: 14615541]

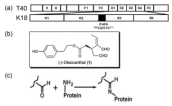

Fig. 1.

Human tau constructs, structure of oleocanthal and Schiff base reaction between oleocanthal and lysine side chain. (a) Schematic representation of human tau constructs. The top bar shows the longest tau isoform T40 (441 amino acids). The C-terminal half of tau contains three or four pseudorepeats (~31 residues each, R1-R4), which constitute the MT-binding domain together with their proline-rich flanking regions (P). ^{306}VQIVYK^{311} (designated as PHF6) at the beginning of R3 (solid) is established to be critical for PHF formation. Construct K18 comprises only the four repeats (R1-R4). (b) Structure of (-)-oleocanthal. (c) Scheme of Schiff base reaction between aldehyde and the ε-amino group of lysine side chain in a protein.

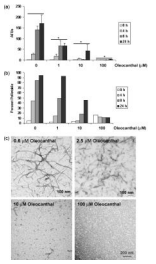

Fig. 2.

Oleocanthal inhibits K18 fibrillization. (a) ThT fluorescence assay of the filament assembly of K18 in the presence of 0-100 μM oleocanthal. *AFUs*, arbitrary fluorescence units. *Error bars* represent S.D.; n=3. *, $P < 0.0001$ vs. 0 μM oleocanthal, two-way ANOVA analysis followed by Bonferroni post-tests. (b) Sedimentation analysis of the filament assembly of K18 in (a). Tau proteins in the supernatants and pellets were quantified by densitometry of the Coomassie blue-stained gels. (c) Negative staining EM of the 16 (0.6 μM and 2.5 μM oleocanthal) or 24-hr samples of K18 assembled in (a) (10 μM and 100 μM oleocanthal). The scale bar for 100 μM oleocanthal also applies to 10 μM oleocanthal.

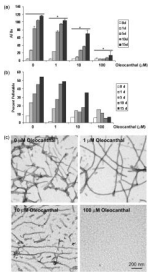

Fig. 3.

Oleocanthal inhibits T40 fibrillization. (a) ThT fluorescence assay of the filament assembly of T40 in the presence of 0-100 μM oleocanthal. *AFUs*, arbitrary fluorescence units. *Error bars* represent S.D.; n=3. *, $P < 0.0001$ vs. 0 μM oleocanthal, two-way ANOVA analysis followed by Bonferroni post-tests. (b) Sedimentation analysis of the filament assembly of T40 in (a). Tau proteins in the supernatants and pellets were quantified by densitometry of the Coomassie blue-stained gels. (c) Negative staining EM of the 24-hr samples of T40 assembled in (a).

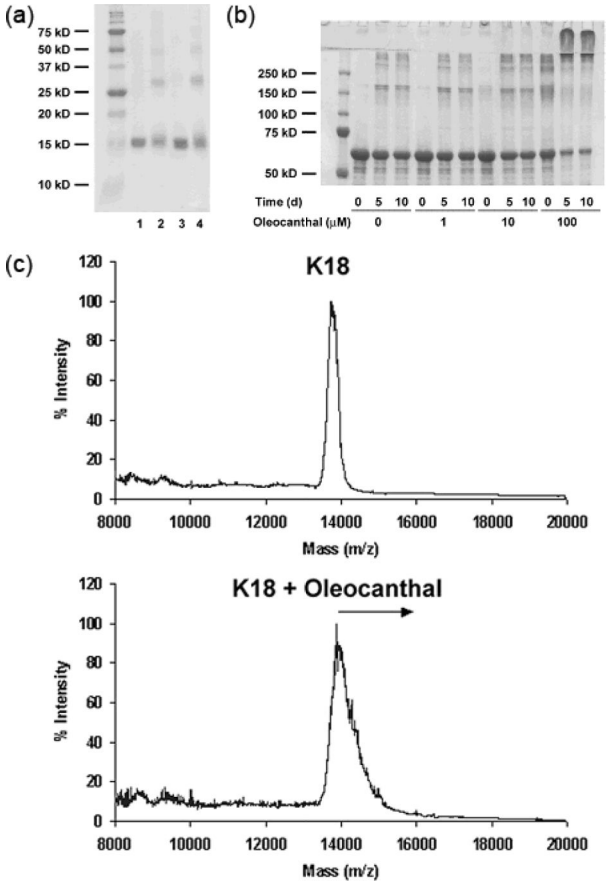

Fig. 4.

Oleocanthal covalently modifies tau. (a) SDS-PAGE analysis of 20 μM K18 incubated without (1, 3) or with (2, 4) 100 μM oleocanthal for 8 hrs (1, 2) or 24 hrs (3, 4). (b) SDS-PAGE analysis of 20 μM T40 assembled in the presence of 0-100 μM of oleocanthal. (c) MALDI analysis of oleocanthal modified K18 indicates mass increase. 20 μM K18 was incubated with 100 μM oleocanthal in 10 mM NaOAc buffer, pH 7.0 at 37 °C for 8 hrs, then mixed with equal volume of 100 mM ammonium bicarbonate buffer, pH 7.7. Samples were diluted 5 fold and spotted on a gold plate for MALDI.

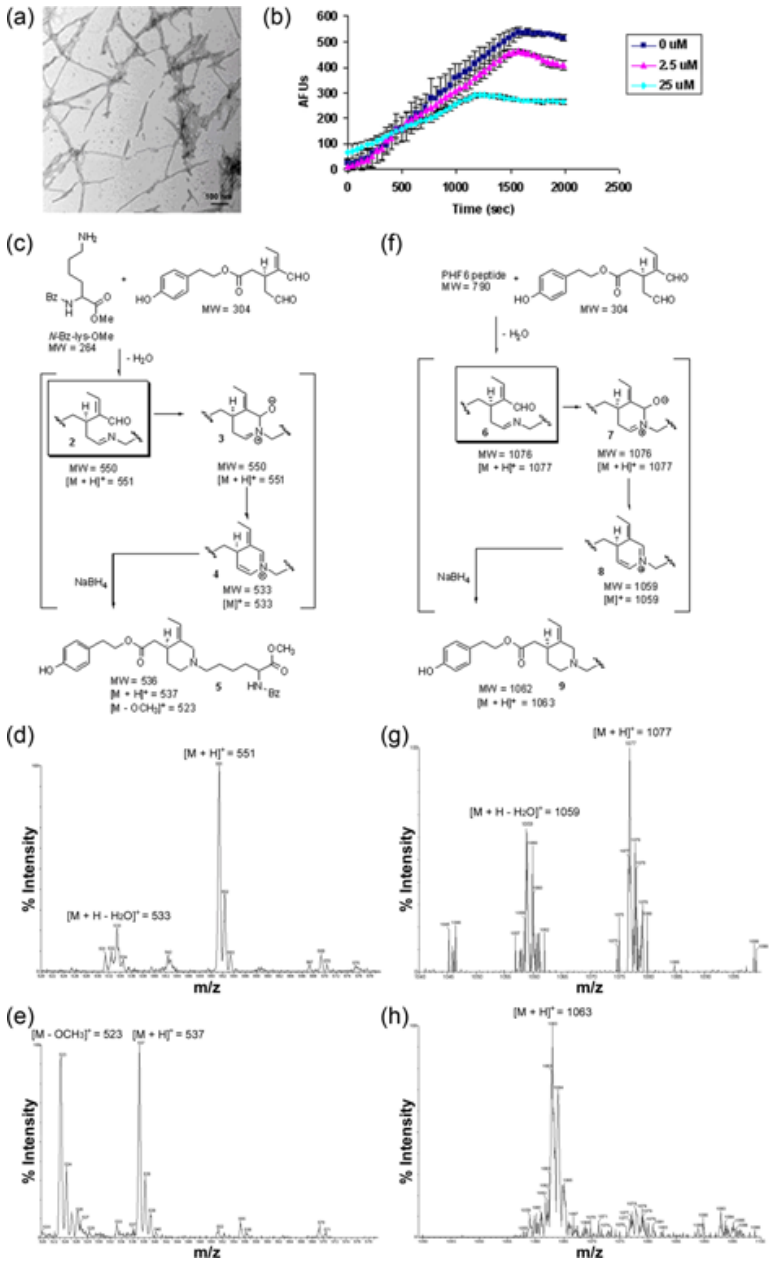

Fig. 5.

Oleocanthal inhibits polymerization of PHF6 peptide via formation of a Schiff base with the lysine side chain. (a) Negative staining EM of paired helical fibrils formed by PHF6 peptide, similar to K18 and T40. 200 μM PHF6 peptide was incubated in 20 mM MOPS buffer, pH 7.2, 150 mM NaCl and 6.25% DMSO at 37 °C for 24 hrs and then used for negative staining. (b) ThT fluorescence assay of the polymerization of PHF6 peptide in the presence of oleocanthal. Polymerization of 2 μM PHF6 peptide in 20 mM MOPS buffer, pH 7.2 with 0-25 μM of oleocanthal was initiated by addition of equal volume of 300 mM NaCl and 20 mM ThT in 20 mM MOPS buffer, pH 7.2. The assembly was conducted in 96 well plates with 100 μL in each well. (c) Chemical reaction of oleocanthal with *N*-Bz-Lys-OMe. (d) LC-MS analysis of reaction between oleocanthal and *N*-Bz-Lys-OMe in methanol before reduction with sodium borohydride. (e) LC-MS analysis of reaction between oleocanthal

and *N*-Bz-Lys-OMe in methanol after reduction with sodium borohydride. (f) Chemical reaction of oleocanthal with PHF6 peptide. (g) LC-MS analysis of reaction between oleocanthal and PHF6 peptide in methanol before reduction with sodium borohydride. (h) LC-MS analysis of reaction between oleocanthal and PHF6 peptide in methanol after reduction with sodium borohydride.

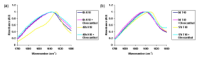

Fig. 6.

Oleocanthal modification blocks the random coil to β-sheet conformational change of tau required for fibrillization. (a) FTIR spectra of K18 assembled for 48 hrs with/without the presence of oleocanthal. (b) FTIR spectra of T40 assembled for 17 days with/without the presence of oleocanthal.

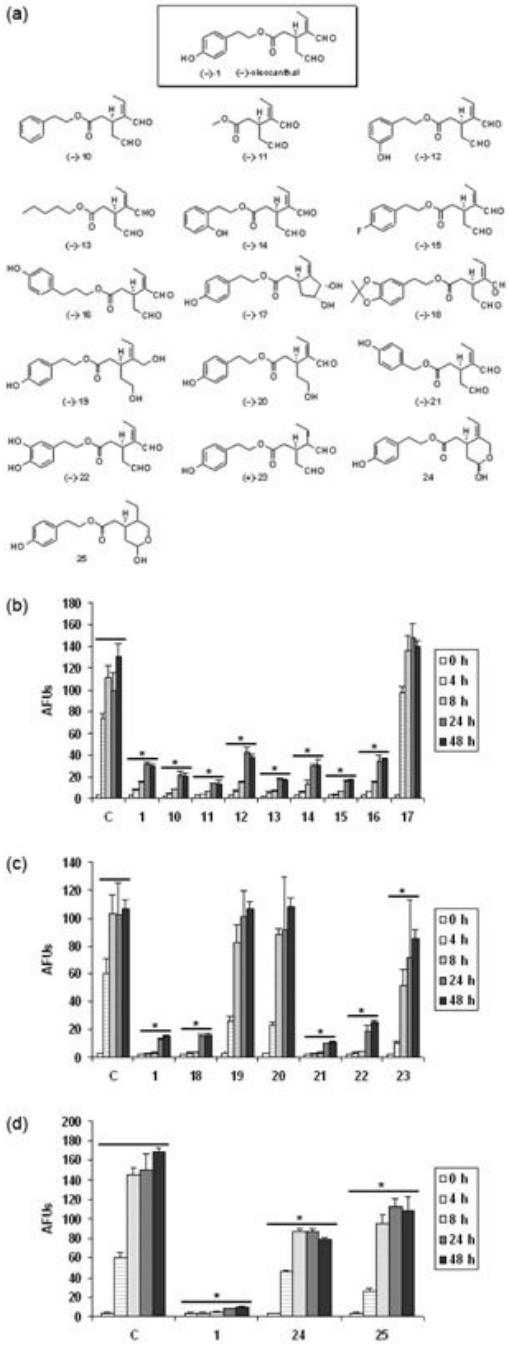

Fig. 7.

Structure-activity relationship studies of oleocanthal and analogues. (a) Structures of oleocanthal analogues synthesized. (b, c, d) Effect of oleocanthal analogues on K18 fibrillization as monitored by ThT fluorescence assay. 10 μM compound is applied to the assembly of 20 μM K18 as described in "Material and methods". *C*, control treated with only vehicle. *AFUs*, arbitrary fluorescence units. *Error bars* represent S.D.; n=3. *, $P < 0.0001$ vs. control treated with only vehicle, two-way ANOVA analysis followed by Bonferroni post-tests.

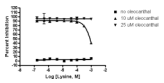

Fig. 8.

Oleocanthal inhibits K18PL fibrillization in the presence of lysine. 0.158 μM to 1 mM lysine was added to the fibrillization of 20 μM K18PL. The reaction was incubated for 6 hrs at 37 °C and the fibrillization was measured by ThT fluorescence. *Error bars* represent S.D.; n=3.

Table 1

Inhibition of PHF6 peptide polymerization by oleocanthal

[Oleocanthal], μM	Rate of polymerization, AFU/sec	Maximum ThT reading, AFU
0	0.36	535
2.5	0.31	464
25	0.19	292

Rate of polymerization is derived from kinetics for the first 1215 seconds through linear regression.